

FLIM Analysis using the Phasor Plots

Shih-Chu Liao, Yuansheng Sun, Ulas Coskun
ISS, Inc.

1 Introduction

Given a number N_0 of molecules in the excited state at time $t = 0$, the fluorescence decay time is the time it takes for the population to decrease by e^{-1} , or about 36.8% of the initial value. The process is accomplished with the emission photons, or fluorescence. The natural fluorescence lifetime of a fluorophore in the absence of non-radiative processes is an intrinsic property of the fluorophore. The fluorescence lifetime of a fluorescent molecule carries information about its local microenvironment and can be very sensitive to certain environmental changes. Therefore, cellular responses to events such as changes in temperature, pH, and ion concentrations (e.g. Calcium) can be measured accurately using Fluorescence Lifetime Imaging Microscopy (FLIM). FLIM is now routinely used for dynamic measurements of signaling events inside living cells, including detection of protein-protein interactions (1).

The traditional approach for the fluorescence time determination consists in using the least-square fitting analysis at each pixel or each group of binned pixels in the image. This approach requires indeed some level of expertise in the choice of the fitting model and a full appreciation of the statistical tools that are to be utilized in cases that are at best disputable. The process can be time consuming for a large amount of data since it typically runs on a pixel-by-pixel basis. Also, the process can easily bring to inaccuracies in the determination of decay times when several decay processes are present, as it is commonly the case for cell biology. In comparison, the phasor plot analysis approach streamlines the procedure and allows for the quantitative determination of fluorescence lifetimes and even Förster resonance energy transfer (FRET) efficiencies. Please see our application note [“The ultimate phasor plot and beyond”](#) for a list of merits of the phasor plot with examples.

2 The non-linear least square fitting

In fluorescence lifetime imaging, the decay times of fluorophores are determined at each spatial location of an image. Assuming an infinite short excitation pulse (δ -function), an intrinsic fluorescence decay composed of N ($N \geq 1$) fluorescent species with distinct fluorescence lifetimes can be modeled by Eq. [1].

$$\hat{I}(t) = \hat{I}(0) \sum_{i=1}^N \alpha_i e^{-t/\tau_i} \quad [1]$$

Where $\hat{I}(0)$ is the number of the instantly emitted photons at time zero; the coefficient α_i , called the pre-exponential factor, is the amplitude and τ_i is the fluorescence decay time of the i th component of the mixture. The

amplitude weighted lifetime τ_a (often called apparent lifetime) given by Eq. [2] is typically used for the calculation of the energy transfer efficiency. The average lifetime $\langle \tau \rangle$ is given by Eq. [3], where f_i is the fractional contribution of the i th species to the total intensity

$$\tau_a = \sum_{i=1}^N \alpha_i \tau_i \quad [2]$$

$$\langle \tau \rangle = \sum_{i=1}^N f_i \tau_i \quad f_i = (\alpha_i \tau_i) / \tau_a \quad [3]$$

Due to the finite response of a system, the measured decay signal $I(t)$ is a convolution form of the intrinsic decay and the instrument response function (*IRF*) plus the noise $n(t)$, as shown in Eq. [4].

$$I(t) = IRF \otimes \hat{I}(t) + n(t) = IRF \otimes \left\{ \hat{I}(0) \sum_{i=1}^N \alpha_i e^{-t/\tau_i} \right\} + n(t) \quad [4]$$

Thus, accurate FLIM data analysis typically requires the calibration of the IRF. In time-domain FLIM, the IRF can be measured by recording the scattered excitation light when using one-photon excitation, or the second-harmonic generation (SHG) signals for two-photon excitation by using a sample that yields strong SHG, such as urea crystal. In frequency-domain FLIM, the IRF is typically calibrated with a fluorescence lifetime standard of known lifetime. A list of these standards is given on the ISS website.

- http://www.iss.com/resources/reference/data_tables/FL_LifetimeStandards.html
- http://www.iss.com/resources/reference/data_tables/LifetimeDataFluorophores.html

Most FLIM data analysis routines involve fitting of the measured data based on a specified decay kinetics model (Eq. [1]). An iteratively constrained optimization algorithm is typically applied to estimate the fitting parameters, i.e. lifetime(s) and pre-exponential factor(s) – at each iteration step, the result calculated from the estimated parameters based on the decay model is compared to the measured data, providing a feedback for updating the fitting parameters as well as a criterion for terminating the iterative optimization process. Through the years several optimization approaches have been used, and a partial list includes: the non-linear least square analysis, the method of moments, maximum entropy, the Laplace transform, the phase plane, the Prony's method, the sine transform, maximum likelihood expectation minimization. For statistical robustness, the method of choice is today the non-linear least square analysis in both time- and frequency-domain analysis.

An important criterion to assess the goodness of the fit for the non-linear least square analysis is the calculated chi-square. In the VistaVision software by ISS, the chi-square functions for both time-correlated single-photon counting (TCSPC) and frequency-domain (FD) FLIM data fitting are minimized using the Levenberg-Marquardt algorithm, as shown below.

2.1 Definition of Chi-Square χ^2 for TCSPC FLIM data

The observable to be measured in TCSPC FLIM is the number of photons in each acquisition bin (N).

The reduced χ^2 function is defined by Eq. [5]:

$$\chi^2 = \frac{1}{n-p-1} \sum_{k=1}^n \frac{[N(t_k) - N_c(t_k)]^2}{\sigma_k^2} = \frac{1}{n-p-1} \sum_{k=1}^n \frac{[N(t_k) - N_c(t_k)]^2}{N(t_k)} \quad [5]$$

Where n is the number of acquisition bins; p is the number of the fitting parameters; $N(t_k)$ is the number of photons collected and $N_c(t_k)$ is the number of photons calculated from the estimated fitting parameters based on the chosen decay model, in each data acquisition bin k ; σ_k is the standard deviation, and for a large number of photon counts following the Poisson distribution it is equal to the square root of $N(t_k)$.

2.2 Definition of Chi-Square χ^2 for FD FLIM data

The observables to be measured in FD FLIM are, for each modulation frequency ω , the phase delay (φ) and the amplitude modulation ratio (m). The reduced χ^2 function is defined by Eq. [6]:

$$\chi^2 = \frac{1}{2n-p-1} \left\{ \sum_{k=1}^n \left[\frac{\varphi_k - \varphi_{ck}}{\sigma_{\varphi k}} \right]^2 + \sum_{k=1}^n \left[\frac{m_k - m_{ck}}{\sigma_{mk}} \right]^2 \right\} \quad [6]$$

Where n is the number of modulation frequencies; p is the number of the fitting parameters; φ_k and m_k are the measured phase shift and modulation ratio, while φ_{ck} and m_{ck} are the calculated phase shift and modulation ratio using the estimated fitting parameters based on the selected decay model, at frequency k ; $\sigma_{\varphi k}$ and σ_{mk} are the uncertainties in the phase and modulation ratio values, respectively. It should be noted that the digital FD (DFD) FLIM approach implemented in ISS FastFLIM carries out multi-modulation-frequency measurements simultaneously, allowing much faster data acquisition than the traditional FD FLIM methods, which measure at multiple frequencies in a sequential way.

2.3 Challenges in the non-linear least square fitting for FLIM data analysis

Using the non-linear least-square fitting for FLIM data analysis, the approach utilized by the user typically encompasses the following sequential steps:

- Establish a decay model such as the N value in Eq. [1]; In most cases, one first starts from the simplest model, i.e. the single exponential decay;
- Make initial guesses to the physical parameters such as α_i and τ_i in Eq. [1] and specify their constraints such as the range of each value upon known priori information.

- Click the “fit” button in the software to let the computer algorithm estimate the results.
- Examine the fit by checking the chi-square value and the fitting residuals.
- If the fit is not acceptable, go back to the first step to apply a more complicated decay model, typically by adding one more exponent, and start over...

It is often straightforward to apply the above steps in commercial software, e.g. VistaVision by ISS. Assessing the fit of the FLIM data, however, can still be challenging. Even though the chi-square value provides a quantitative measurement for fitting, there is no golden rule made only based on it to accept or reject a fitting model. This is simply because the photon counts in most of real experiments are limited and far less than the statistical requirement. Therefore, the traditional non-linear fitting for FLIM data analysis indeed requires some level of expertise in understanding the physics of fluorescence lifetime and a full appreciation of the statistical tools that are to be utilized in cases that are at best disputable.

3 The phasor plot

The phasor plot, also known as the AB plot or the polar plot (2-6), is a graphic representation of the raw FLIM data. Transforming FD or TCSPC FLIM data into the phasor plot is described below.

3.1 The phasor plot for FD FLIM data

For one modulation frequency (ω), the FD FLIM data measurements at each pixel location are composed of both the phase delay (φ) and the amplitude modulation ratio (m) (see Figure 1). The FD FLIM data at each pixel can be mapped to a single point called “phasor” in the phasor plot through a transform defined by Eq. [7], where g and s represent the values at the two coordinates (G, S) of the phasor plot.

$$g(\omega) = m \cos(\varphi) \quad \text{and} \quad s(\omega) = m \sin(\varphi) \quad [7]$$

3.2 The phasor plot for TCSPC FLIM data

In TCSPC FLIM, a decay trace $I(t)$ (see Eq. [4]) is recorded at each pixel location; each decay trace can be plotted as a single point (“phasor”) in the phasor plot by applying the sine and cosine transforms to the measured decay data, as shown by Eq. [8] and Figure 1. This is equivalent to the real and imaginary components of the Fourier transform of the decay data.

$$g(\omega) = \frac{\int_0^{\infty} I(t) \cos(\omega t) dt}{\int_0^{\infty} I(t) dt} \quad \text{and} \quad s(\omega) = \frac{\int_0^{\infty} I(t) \sin(\omega t) dt}{\int_0^{\infty} I(t) dt} \quad [8]$$

Where the modulation frequency ω is now called the laser repetition angular frequency and calculated by multiplying the laser repetition rate with 2π .

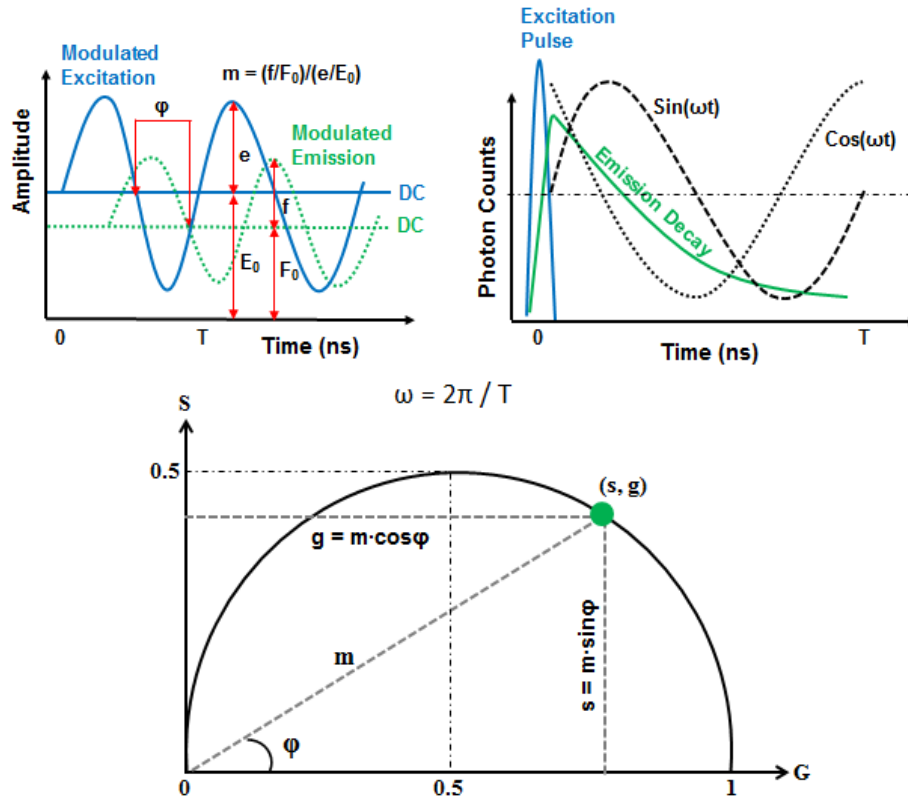


Figure 1: Mapping FD and TCSPC FLIM data to the phasor plot.

3.3 Calibrating the phasor plot

In order to establish the correct scale for the plotted phasor points, the coordinates of the phasor plot need to be calibrated using a standard sample of known lifetime. This is indeed the calibration of the IRF.

- In FD FLIM, this is already done when calibrating the instrument prior to the data acquisition.
- In TCSPC FLIM, this can be done by applying the Fourier transform to a recorded decay trace of known lifetime, e.g. a decay acquired using Fluorescein at pH 9 (4 ns lifetime); alternatively, a directly recorded IRF data trace for the zero lifetime can be used for the Fourier transform.

3.4 Phasor vs. lifetime

By taking Eq. [1] into Eq. [8] and solving the integrals, we can then derive the following relationships between the phasor and the lifetime, given by Eq. [9].

$$g = \sum_{i=1}^N \frac{f_i}{1 + \omega^2 \tau_i^2} \quad \text{and} \quad s = \sum_{i=1}^N \frac{f_i \omega \tau_i}{1 + \omega^2 \tau_i^2} \quad [9]$$

As explained above in Eq. [1-3], N is the number of the fluorescent species, and f_i is the fractional contribution of the i th species of the fluorescence lifetime τ_i to the total intensity.

3.5 The universal semicircle

For a single-lifetime species ($N = 1$), Eq. [9] is reduced to Eq. [10] and the lifetime can be directly determined by the coordinate values of a phasor. It is further derived that the two coordinates of a phasor representing a single-lifetime species must have the relationship given by Eq. [11]. The relationship is drawn as a semicircle curve centering at ($G = 0.5, S = 0$) with a radius of 0.5 in the phasor plot, and this semicircle curve is often called the universal semicircle or the universal trajectory.

$$g = \frac{1}{1 + \omega^2 \tau^2} \quad s = \frac{\omega \tau}{1 + \omega^2 \tau^2} \quad \tau = \frac{1}{\omega} \left(\frac{s}{g} \right) \quad [10]$$

$$(g - 0.5)^2 + s^2 = 0.25 \quad [11]$$

3.6 Decomposition of the phasor of a complex species

For a multiple-lifetime species ($N > 1$), Eq. [9] can be re-written by Eq. [12], given below.

$$g = \sum_{i=1}^N (f_i g_i) \quad \text{and} \quad s = \sum_{i=1}^N (f_i s_i) \quad [12]$$

$$g_i = \frac{1}{1 + \omega^2 \tau_i^2} \quad s_i = \frac{\omega \tau_i}{1 + \omega^2 \tau_i^2} \quad [13]$$

This decomposition demonstrates that a phasor of a complex species (g, s) is a linear combination of multiple phasors, each (g_i, s_i) representing an individual species. Again, f_i is the fractional contribution of the i -th species represented by the phasor (g_i, s_i) to the total intensity. This is a very important property of the phasor plot, making the phasor plot a simple but powerful tool for quantitative FLIM data analysis.

4 The phasor plot analysis

By plotting raw FLIM data in the phasor plot, one can analyze and interpret the data by following a few basic rules of the phasor plot, as discussed below.

4.1 The universal semicircle rules

- **The universal semicircle is a lifetime ruler.** The universal semicircle defined by Eq. [11] becomes an explicit lifetime ruler for single-lifetime species in the phasor plot. For example, [Figure 2](#) displays the lifetimes of Rose Bengal in different solvents. This trajectory also indicates relative changes in lifetime for complex species such that the lifetimes decrease from left (1, 0) being lifetimes near zero to right (0, 0) being infinite lifetimes.

- **The scale of the semicircle ruler is adjustable upon the modulation frequency.** Given the same single-lifetime value, the phasor shifts to the left along the semicircle for a lower modulation frequency “ ω ” which results in an increase of the “s/g” ratio (see Eq. [10]). An example comparing the phasor plots of two modulation frequencies is shown in Figure 3. Thus, the scale of the semicircle ruler can be easily adjusted by changing the modulation frequency to draw the phasor plot, making the phasor plot very flexible to visualize different lifetimes and highlight the contrast upon the lifetime values. Typically, the available modulation frequencies are the integer multiples of the fundamental modulation frequency. The measurements of different modulation frequencies are performed simultaneously by ISS FastFLIM, and choosing a proper modulation frequency to make the phasor plot is as easy as a simple click in the ISS VistaVision software.
- **Single-lifetime species are on the semicircle.** As defined by Eq. [10-11], a phasor point or population falling or centering at a point on the semicircle indicates a single-lifetime specie.
- **Complex species are inside the semicircle.** As defined by Eq. [12], the phasor of a complex species is a linear combination of the individual phasors of single-lifetime species. Connecting these individual phasors on the semicircle yields a convex set inside the semicircle, and thus a species of multiple lifetime components must fall inside the semicircle.
- **Excited-state products are outside the semicircle.** In most FLIM measurements, every fluorescent component contributing the measured lifetime is excited directly by the excitation light and the corresponding phasor should never be outside the semicircle, assuming no perturbation from noise. However, when a fluorescent component is an excited-state product, e.g. the sensitized emission of the acceptor produced by the energy transfer from the excited-state donor in a FRET event, its phasor would locate outside the semicircle.

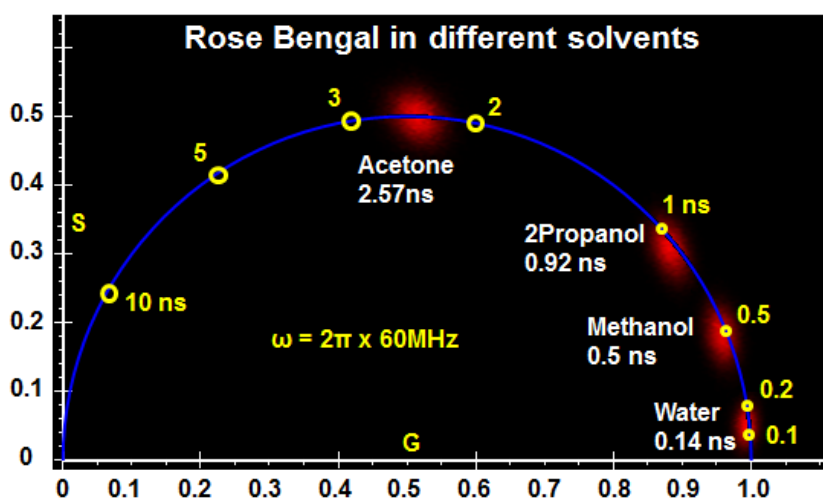


Figure 2: Decay time of Rose Bengal in different solvents displayed in the phasor plot. Data was acquired using the ISS Alba V system using the 561 nm laser excitation. (Courtesy of Dr. Ammasi Periasamy, University of Virginia)

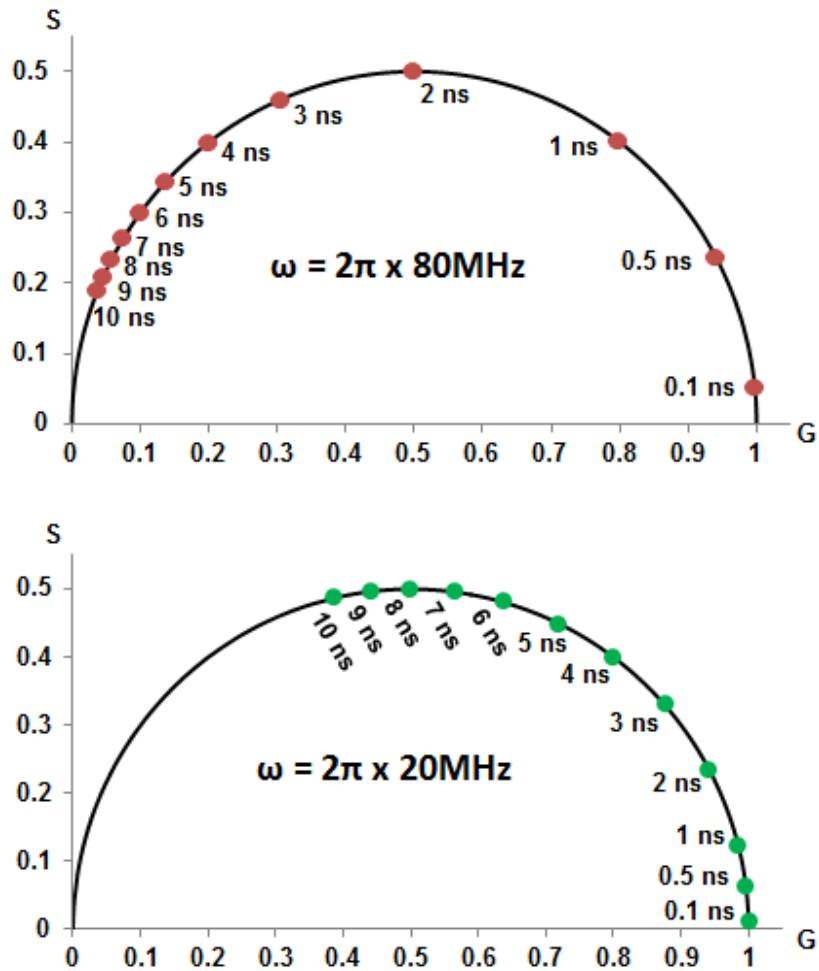


Figure 3: Comparison of the phasor plot scales of two different modulation frequencies.

4.2 The phasor decomposition rules

- Decomposing the phasor of a complex species is a linear process, described by Eq. [12].** As shown in [Figure 4](#), the phasor point of a mixture composed of two species must lie on the line connecting the two phasors of representing each individual species, and the contribution from one species to the mixture is proportional to the distance from the mixture point to the other species point; for more components, the mixture must locate inside the convex set connecting all the phasors of individual species (e.g. a triangle for 3 components). An example of comparing the mixture of two species vs. the two individual species is shown in [Figure 5](#).
- The phasor decomposition is often not to solve the individual single-lifetime components.** It should be noted that the decomposed individual species does not have to be a single-lifetime species, e.g. the A-B mixture case shown in [Figure 4](#), where both species A and B have multiple lifetime components. This is a key concept of using the phasor plot to analyze a complex system, where it is almost impossible to solve individual lifetime components

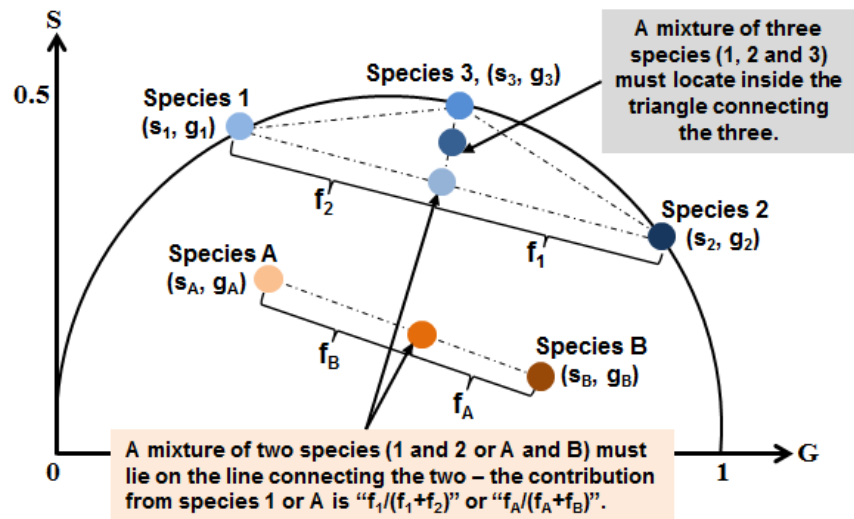


Figure 4: The phasor linear decomposition.

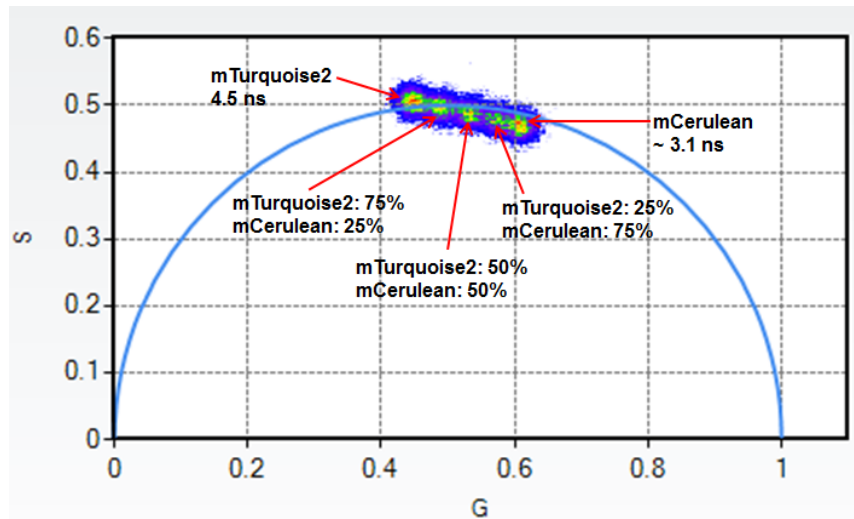


Figure 5: Comparison of mCerulean, mTurquoise2 and three mixtures of the two species in the phasor plot. Data was acquired using the ISS Alba V system using the 440 nm laser excitation source. (Courtesy of Dr. Richard N. Day; Indiana University School of Medicine)

4.3 The FRET trajectory approach for quantitative FRET data analysis

FRET is non-radiative energy transfer from an excited molecule (the donor) to another nearby molecule (the acceptor) through a long range dipole–dipole coupling mechanism. As given by Eq. [13], the efficiency of energy transfer (E) from the donor to the acceptor is dependent on the inverse of the sixth power of the distance separating them (r), subject to their Förster distance (R_0) at which E is 50% (7-8). FRET is typically limited to distances less than about 10 nm, making it a powerful tool for investigating a variety of phenomena that produce changes in molecular proximity.

$$E = \frac{R_o^6}{R_o^6 + r_o^6} \quad \text{and} \quad r = R_o \left(\frac{1-E}{E} \right)^{1/6} \quad [14]$$

FLIM is among the most accurate methods of measuring FRET (1). In a FLIM-FRET experiment, the quenched lifetimes of the donor (τ_{DA}) in the samples containing both the donor and the acceptor are measured to map the FRET efficiencies based on Eq. [14], where the unquenched donor lifetime (τ_D) is typically determined from the donor-only control sample. As only donor signals are measured by FLIM for determining the FRET efficiency, the method does not require the corrections for spectral bleedthrough that are necessary for intensity-based measurements of sensitized emission from the acceptor.

$$E = 1 - \frac{\tau_{DA}}{\tau_D} \quad [15]$$

In the phasor plot, it is easy to visualize the difference of the lifetimes from unquenched vs. quenched donor samples; however, it does not seem to be straightforward to link both the data of both unquenched and quenched donors to produce the FRET efficiency. Fortunately, Dr. Gratton's LFD group came up an elegant solution, called the FRET trajectory approach (2). The basic principle of this approach is illustrated in Figure 6, and is to decompose the quenched donor phasor measured from the donor in the presence of the acceptor into three species:

- **The unquenched donor species with the lifetime of (τ_D)** – the phasor of this species can be measured independently from the donor-only control sample.
- **The background species with an arbitrary lifetime** – the phasor of this species can be determined independently from the unlabeled control sample.
- **The quenched donor species with the lifetime of (τ_{DA})** – its phasor can be calculated for any FRET efficiency value ranging from 0 to 1, given the unquenched donor (τ_D) to Eq. [14].

Given the fraction contribution of each species, the phasor composed of the three species (unquenched donor, the background and the quenched donor) for any FRET efficiency value can be located on the phasor plot – connecting all phasor points corresponding to FRET efficiencies ranging from 0 to 1 makes a trajectory, named FRET trajectory. Each point on the trajectory represents a FRET efficiency value. Both the starting ($E = 0$) and the ending ($E \approx 1$) points of a FRET trajectory are on the line of connecting the unquenched donor and the background phasors, while the starting and the ending positions depend on the fraction contributions of the background and the unquenched donor (see Figure 6):

- When the fraction contribution from the background (f_B) is zero, a FRET trajectory would always start from the unquenched donor phasor point.
- When the fraction contribution from the unquenched donor (f_D) is zero, a FRET trajectory would always ends at the background phasor point.
- Likely, both background and unquenched donor give some fraction contributions – in this case, more fraction contribution given by the background will push the starting point further way from the unquenched donor phasor, and more fraction contribution from the unquenched donor will shift the ending point further way from the background phasor.

The goal now comes to find the FRET trajectory to pass through the measured quenched donor phasor and then simply read its FRET efficiency at the intersection. The ISS VistaVision software makes this a step-by-step routine requiring no expertise, as outlined below:

- Load unquenched (donor-only), background (unlabeled) and quenched (donor + acceptor) data (images) into the phasor plot using the “Multi-Image Phasor Analysis” module (see Figure 7). In this example, the background data is ignored by assuming the zero lifetime for it.
- Select the population of the unquenched donor (Cerulean-alone in this example) phasor points using the circle shown on the phasor plot and assign it to be the unquenched donor phasor position. Use the arrow buttons to finely adjust the circle position, and a higher “Score” indicates a better circle position that matches the selected population. The circle size is adjustable.
- Select the population of the phasor points originated from background using the circle and assign it to be the background phasor position. In this example, the background is assumed to be from the scatter of the excitation light and its phasor position is defined at the ($G = 1, S = 0$) for zero lifetime.
- Click the “FRET Calculator” button in the “Multi-Image Phasor Analysis” module to plot the FRET trajectory (see Figure 7). The trajectory changes upon the fraction contributions from the background and the unquenched donor, each of which is adjusted independently by the users using its sliding bar. The background fraction contribution can often be measured from the unlabeled control sample, leaving only one variable (the fraction contribution from the unquenched donor) to be adjusted to make the FRET trajectory to pass through the measured quenched donor phasor.
- A circle lies on the FRET trajectory and travels along the trajectory by sliding the “Efficiency” (FRET efficiency) bar. By sliding the “Efficiency” value, one can move the circle to the position that best matches the population of the quenched donor (C5V in this example) phasor points – here, its FRET efficiency is obtained from reading the value shown in the “Efficiency” bar. A fine adjustment of the fraction contribution from the unquenched donor may be applied to improve the result accuracy. Again, a higher “Score” indicates a better circle position that matches the selected population and the circle size is adjustable.

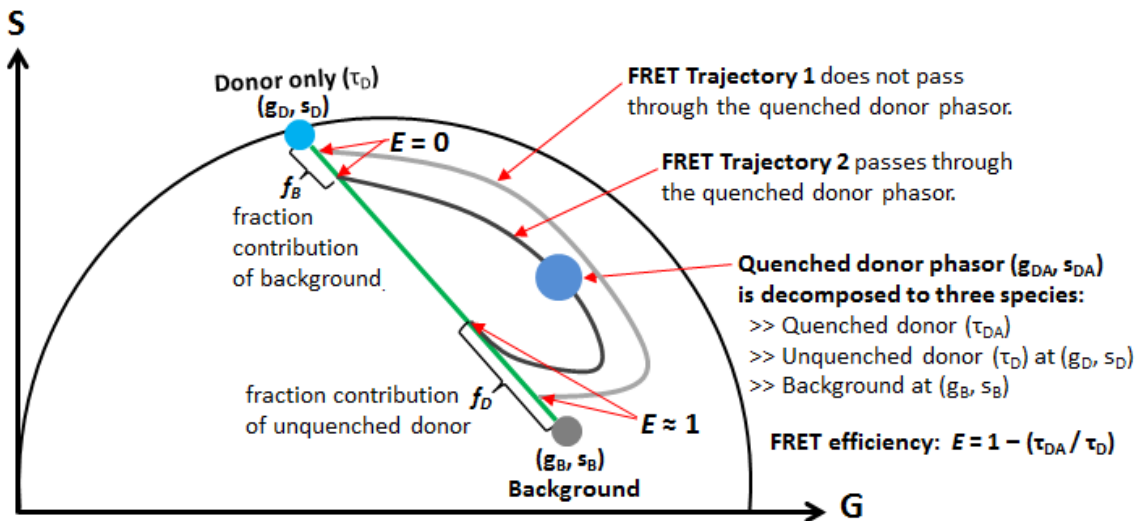


Figure 6: The phasor plot FRET trajectory approach.

- Notes:** The data was acquired using live cells expressing Cerulean-alone (unquenched donor) and the FRET-standard construct C5V (quenched donor), developed by the Vogel's laboratory at NIH/NIAAA through encoding fusions between Cerulean (FRET donor) and Venus (FRET acceptor) fluorescent proteins separated by a 5 amino acid linker (9).

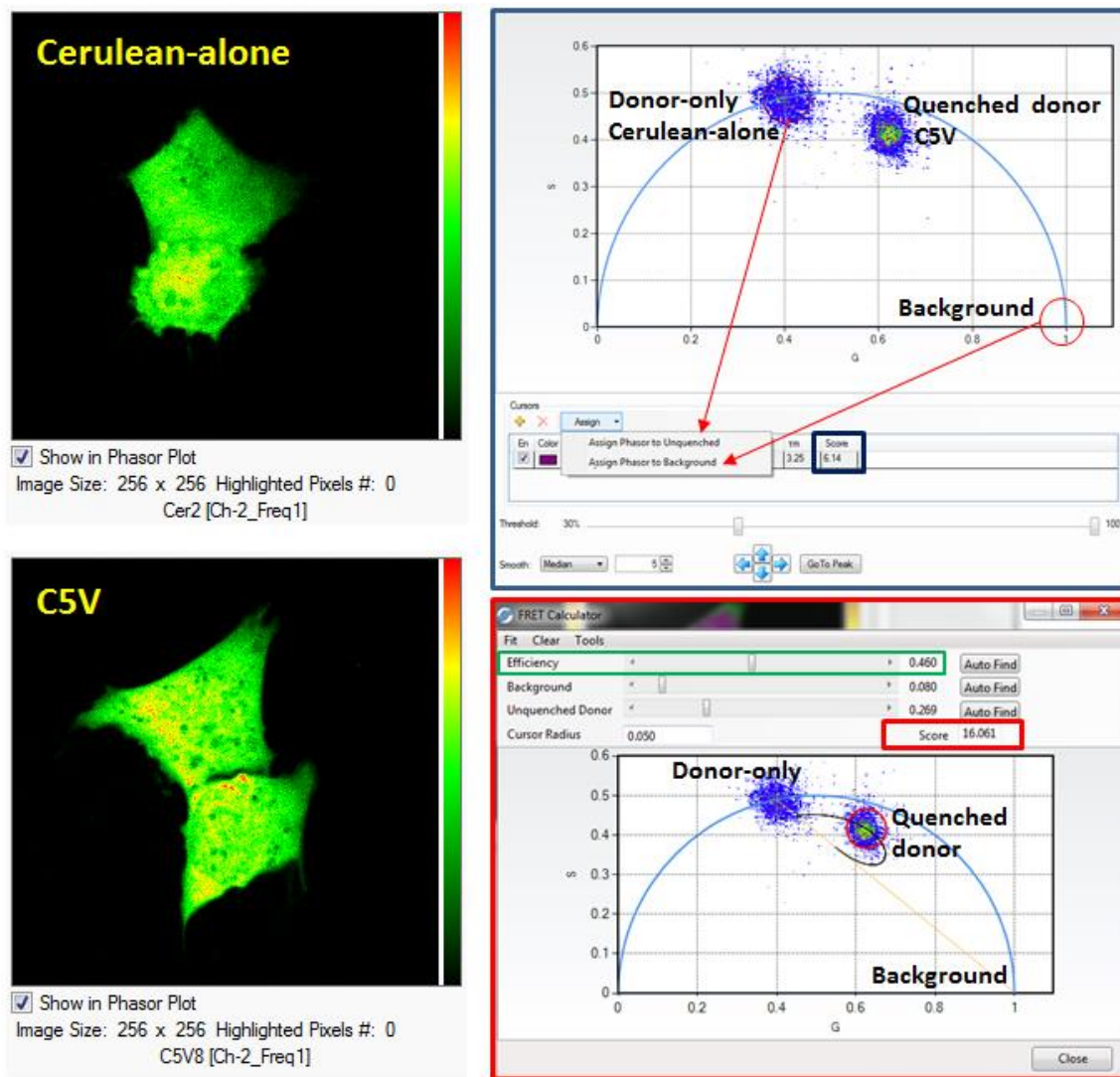


Figure 7: Determine the FRET efficiency using the “FRET trajectory” approach in the ISS VistaVision software.

References

- Sun, Y., R.N. Day and A. Periasamy 2011. *Investigating protein-protein interactions in living cells using fluorescence lifetime imaging microscopy*. Nat. Protoc. 6, 1324-1340.
- Digman, M. A., V.R. Caiolfa, M. Zamai and E. Gratton 2008. The phasor approach to fluorescence lifetime imaging analysis. Biophys. J. 94, L14-6.

3. Stringari, C., A. Cinquin, O. Cinquin, M.A. Digman, P.J. Donovan and E. Gratton 2011. Phasor approach to fluorescence lifetime microscopy distinguishes different metabolic states of germ cells in a live tissue. *Proc. Natl. Acad. Sci. U. S. A.* 108, 13582-13587.
4. Redford, G. I. and R.M. Clegg 2005. Polar plot representation for frequency-domain analysis of fluorescence lifetimes. *J. Fluoresc.* 15, 805-815.
5. Clayton, A. H., Q.S. Hanley and P.J. Verveer 2004. Graphical representation and multicomponent analysis of single-frequency fluorescence lifetime imaging microscopy data. *J. Microsc.* 213, 1-5.
6. Hanley, Q. S. and A.H. Clayton 2005. AB-plot assisted determination of fluorophore mixtures in a fluorescence lifetime microscope using spectra or quenchers. *J. Microsc.* 218, 62-67.
7. Förster, T.1965. *Delocalized excitation and excitation transfer*, In *Modern quantum chemistry*, Sinanoglu, O., editors. Academic Press Inc., 93-137.
8. Clegg, R. M.1996. *Fluorescence resonance energy transfer*. In *Fluorescence imaging spectroscopy and microscopy*, Wang, X. F., Herman, B., editors. John Wiley & Sons Inc., New York. 179-251.
9. Koushik, S. V., H. Chen, C. Thaler, H.L. Puhl 3rd and S.S. Vogel 2006. *Cerulean, Venus, and VenusY67C FRET reference standards*. *Biophys. J.* 91, L99-L101.

For more information please call (217) 359-8681
or visit our website at www.iss.com



ISSTM

1602 Newton Drive
Champaign, Illinois 61822 USA
Telephone: (217) 359-8681
Fax: (217) 359-7879
Email: iss@iss.com

© Copyright 2014 ISS Inc. All rights reserved, including those to reproduce this article or parts thereof in any form without written permission from ISS. ISS, the ISS logo are registered trademarks of ISS Inc.